

# Physical-Layer Security in MCF-based SDM-EONs: Would Crosstalk-Aware Service Provisioning be Good Enough?

Jing Zhu and Zuqing Zhu, *Senior Member, IEEE*

**Abstract**—In this paper, we consider a multi-core fibers (MCFs) enabled elastic optical network (EON) in which certain nodes have a lower trust-level than the others, and study how to provision lightpaths with considerations of the impairments and security vulnerabilities caused by inter-core crosstalk. We propose attack-aware routing, spectrum and core assignment (Aa-RSCA) algorithms that give priority to avoiding physical-layer security threats and then try to reduce the crosstalk-induced impairments. Specifically, both static network planning and dynamic network provisioning are investigated. For static planning, we first formulate an integer linear programming (ILP) model to optimize the spectrum utilization and inter-core crosstalk level jointly, and then propose a time-efficient heuristic. Simulation results confirm that the proposed heuristic can approximate the ILP's performance with much higher time-efficiency in a small-scale network, and outperform an existing benchmark in large networks. For dynamic provisioning, we design a heuristic to balance the tradeoff between blocking probability and crosstalk, and conduct extensive simulations to verify its effectiveness.

**Index Terms**—Elastic optical networks (EONs), Multi-core fibers (MCFs), Inter-core crosstalk, Physical-layer security.

## I. INTRODUCTION

**D**UE to the fast development of bandwidth-hungry network applications, the traffic in backbone networks is growing exponentially, which is challenging the capacity, efficiency and adaptivity of optical networks intensively. Under this circumstance, elastic optical networks (EONs) have attracted a lot of research interests recently since they can provide flexible bandwidth management with sub-wavelength granularity (*i.e.*, 12.5 GHz or even smaller) in the optical layer [1, 2]. Specifically, unlike the traditional fixed-grid wavelength-division multiplexing (WDM) networks, EONs, with the assistance of bandwidth-variable transponders (BV-Ts) and wavelength selective switches (BV-WSS'), manage optical spectrum in the form of narrow-band frequency slots (FS') and allocate bandwidth in a flexible grid [3, 4]. Hence, they can support not only sub-wavelength channels but also super-channels. Meanwhile, space-division multiplexing (SDM) based on multi-core fibers (MCFs) have been demonstrated recently to further expand fiber capacity [5]. An MCF consists of multiple cores, each of which carries optical signals as a single-core fiber does. Therefore, the transmission capacity can be significantly improved to over Pbit/s per fiber [6].

Although SDM and EON are orthogonal, a symbiosis of them (*i.e.*, SDM-EON) could not only provide expanded fiber capacity but also enable flexible and adaptive bandwidth allocation. When it comes to MCF-based SDM-EONs, the basic routing and spectrum assignment (RSA) problem in EONs [7–12] gets transformed into the routing, spectrum and core assignment (RSCA) problem [13, 14]. As there is one additional dimension (*i.e.*, core assignment) to handle, RSCA is intrinsically more complex than RSA. Moreover, it is known that in MCF-based SDM-EONs, inter-core crosstalk can affect the quality-of-transmission (QoT) of lightpaths significantly [5], which would further complicate the RSCA problem. Hence, to tackle RSCA, the approaches developed for RSA were revisited and improved to realize a few crosstalk-aware service provisioning schemes for reducing the negative effects of inter-core crosstalk in SDM-EONs [13–15].

Note that, there would be physical-layer vulnerabilities in optical networks, if lightpaths with different trust-levels share network elements unrestrictedly [16]. Specifically, the crosstalk among lightpaths that share fiber links and/or optical switches can be leveraged by malicious clients to launch physical-layer attacks [17, 18]. For instance, a malicious client can launch a jamming attack by injecting high power light deliberately to degrade the QoT of normal lightpaths, or set up a lightpath to transmit unmodulated light and collect crosstalk-induced leakage from neighboring channels for eavesdropping. Unfortunately, compared with WDM networks and traditional EONs, MCF-based SDM-EONs have more intimidating physical-layer vulnerabilities for two reasons: 1) the inter-core crosstalk is a new type of crosstalk that has not been considered before, and 2) the usage of spectral/spatial super-channels makes the traffic loss more severe if a lightpath gets disturbed/compromised. Therefore, when setting up lightpaths in an SDM-EON, we might not just maintain the crosstalk-level below a predefined threshold as proposed in [13, 14]. This is because if the predefined threshold is relatively low, it is only good enough to avoid the negative effects of crosstalk among trusted lightpaths but become insufficient to address the deliberate attacks (*e.g.*, power jamming); otherwise, if we set the threshold high enough to prevent any physical-layer attacks, it would be overkill for trusted lightpaths, causing unnecessary spectrum wastage and fragmentation [19–21]. Hence, the RSCA scheme in SDM-EONs should treat trusted and untrusted lightpaths in a differentiated way to improve spectrum utilization while maintaining the network's security level. Nevertheless, to the best of our knowledge, this has not

J. Zhu and Z. Zhu are with the School of Information Science and Technology, University of Science and Technology of China, Hefei, Anhui 230027, P. R. China (email: zqzhu@ieee.org).

Manuscript received on July 20, 2017.

been studied before.

In this work, we consider an SDM-EON in which certain nodes have a lower trust-level than the others (*i.e.*, can be used to launch malicious lightpaths), and study how to provision lightpaths in such a network with considerations of the impairments and security vulnerabilities caused by inter-core crosstalk. We propose attack-aware RSCA (Aa-RSCA) algorithms that give priority to avoiding physical-layer security threats and then try to reduce the crosstalk-induced impairments. Specifically, both static planning and dynamic provisioning scenarios are investigated. For static planning, we formulate an integer linear programming (ILP) model to optimize the spectrum efficiency and crosstalk jointly, and then propose a time-efficient heuristic. Simulation results demonstrate that the heuristic could approximate the ILP's performance in a small-scale network and outperform the benchmark in larger networks. For dynamic provisioning, we also design a heuristic algorithm and extensive simulations verify its effectiveness.

The rest of the paper is organized as follows. Section II provides a brief survey on the related work. The problem description is given in Section III. In Section IV, we formulate the ILP model for static planning and in Section V, a time-efficient heuristic is proposed. Section VI presents the performance evaluation for static planning. In Section VII, we propose an algorithm for dynamic provisioning and discuss its performance. Finally, Section VIII summarizes the paper.

## II. RELATED WORK

Since the impacts of certain physical-layer attacks (*e.g.*, power jamming and wiretapping) can hardly be compensated or even detected by upper-layer applications, physical-layer security should never be overlooked in optical networks [16, 22]. In addition to developing new hardware for attack avoidance and fault management [23–26], people also tried to minimize the damages caused by potential physical-layer attacks via careful network planning and/or service provisioning.

For WDM networks, attack-aware routing and wavelength assignment (Aa-RWA) schemes were studied in [17, 27–29]. In [27], the authors considered the security threat from the intra-channel crosstalk generated by non-ideal port isolation in optical switches, and proposed a wavelength assignment scheme to limit the maximal propagation of the attacks that leverage such crosstalk. Then, in [28], they improved the scalability of their proposal. With consideration of the maximum lightpath attack radius, Skorin-Kapov *et al.* [17] solved the routing subproblem to address the physical-layer vulnerabilities induced by inter-channel crosstalk. The attack-aware routing and wavelength assignment subproblems were considered jointly in [29]. In single-core fiber based EONs, since the channel spacing can be much narrower than that in WDM networks, attack-aware RSA (Aa-RSA) schemes become more challenging. Therefore, we considered the security threats from alien lightpaths in the multi-domain scenario, and proposed a few Aa-RSA algorithms in [18]. Then, with the assistance of game theory, we improved our proposals to achieve a better tradeoff between spectrum utilization and

security level in [30]. However, all these existing studies on attack-aware network planning and service provisioning were targeted for optical networks based on single-core fibers, and did not consider the inter-core crosstalk related attack scenarios in MCF-based optical networks.

Meanwhile, people have also investigated crosstalk-aware network planning and service provisioning schemes for MCF-based SDM-EONs. In [31], the authors leveraged the coupled-mode and coupled-power theory to come up with a mathematical model for estimating inter-core crosstalk. Then, Fujii *et al.* [15] simplified the model for estimating inter-core crosstalk and developed a core prioritization mechanism that utilizes non-adjacent cores to reduce the crosstalk among lightpaths in a best-effort way. However, since the best-effort scheme cannot guarantee sufficient crosstalk suppression among trusted and untrusted lightpaths, the crosstalk-aware service provisioning in [15] cannot address the physical-layer vulnerabilities in MCF-based SDM-EONs properly. The work in [32] first precalculated the inter-core crosstalk among routing paths in the worst-case scenario, and then designed a crosstalk-aware RSCA scheme that can maintain the crosstalk among provisioned lightpaths below a predefined threshold. Nevertheless, as the crosstalk suppression between two trusted lightpaths and that between trusted and untrusted ones should be different, this scheme would be overkill for trusted lightpaths and could cause unnecessary spectrum wastage and fragmentation. In [14], the authors proposed to check the crosstalk-level of all established lightpaths before setting up a new one, which was done by maintaining three tables to track the network status constantly. However, since it is based on exhaustive search, the proposed scheme may have scalability issues.

## III. PROBLEM DESCRIPTION

We model the topology of an MCF-based SDM-EON as  $G(V, E)$ , where  $V$  and  $E$  represent the sets of nodes and bidirectional MCF links, respectively. In the topology, certain nodes have a lower trust-level than the others and they are treated as the potential source nodes of malicious lightpaths. We use  $V_l \subset V$  to denote the set of these untrusted nodes. An MCF  $e \in E$  consists of  $N$  cores, each of which can carry  $F$  frequency slots (FS'). The bandwidth of an FS is 12.5 GHz. A lightpath request is  $L_i(s_i, d_i, n_i)$ , where  $i$  is its unique index,  $s_i$  and  $d_i$  represent its source and destination nodes in  $V$ , respectively, and  $n_i$  is its bandwidth demand in number of FS'. Apparently, if  $s_i \in V_l$ ,  $L_i$  will be considered as an untrusted lightpath, and a trusted one otherwise<sup>1</sup>. To simplify the problem, we assume that each  $L_i$  uses the shortest routing path  $P_i$ . To provision  $L_i$ , we need an attack-aware RSCA (Aa-RSCA) algorithm that can select a core on each  $e \in P_i$  and assign  $n_i$  FS' on each selected core under the spectrum non-overlapping, contiguous and continuity constraints [33–35]. Note that, to realize a highly-flexible SDM-EON, we assume that each node in  $V$  has the capability of core switching [5], *i.e.*, different cores can be selected on the MCFs along  $P_i$ .

<sup>1</sup>Here, we consider a transparent optical network in which optical-electrical-optical conversions would not be conducted in the middle of any lightpath. Hence, a lightpath's trust-level is determined by that of its source node.

It is known that when two lightpaths (e.g.,  $L_i$  and  $L_j$ ) whose spectrum assignments overlap with each other are allocated to neighboring cores in an MCF, there will be inter-core crosstalk between them [15]. Therefore, if  $L_i$  and  $L_j$  are in different trust-levels, we should avoid assigning them to neighboring cores in a same MCF if their spectrum assignments are overlapped, for eliminating the possibility of the untrusted lightpath launching physical-layer attacks by leveraging inter-core crosstalk. Otherwise, if they have the same trust-level, the spectrum overlapping in neighboring cores is considered to cause normal impairments only and thus we only need to reduce the negative effects in a best-effort way, for improving spectrum utilization. To address this problem, we will consider both static network planning and dynamic network provisioning and design several Aa-RSCA algorithms in this work. For static planning, we try to improve spectrum utilization and reduce inter-core crosstalk jointly, while in dynamic provisioning, we aim at balancing the tradeoff between blocking probability and crosstalk-level.

Fig. 1 shows an example on Aa-RSCA in an MCF-based SDM-EON. The topology of the SDM-EON in Fig. 1(a) indicates that *Nodes* 1 and 4 are untrusted ones (i.e.,  $V_i = \{1, 4\}$ ), and there are three lightpaths, i.e.,  $L_1(1, 3, 2)$ ,  $L_2(2, 3, 3)$ , and  $L_3(6, 3, 4)$  to be established. The lightpaths' routing paths are determined as shown in Fig. 1(a), all of which traverse *Link* 2→3. For simplicity, we assume that each MCF has the layout of a 3-core linear array in a rectangle [5], as illustrated in Fig. 1(b). The cores are numbered for prioritization [15], and we can see that *Core* 3 is adjacent to *Cores* 1 and 2, while *Cores* 1 and 2 are non-adjacent. Two feasible Aa-RSCA solutions are plotted in Figs. 1(c) and 1(d), respectively. In Fig. 1(c), since  $L_1$  and  $L_3$  are in different trust-levels and use *Cores* 1 and 3, respectively, their spectrum assignments cannot overlap. On the other hand, as  $L_2$  and  $L_3$  are both trusted ones, they can use overlapped spectrum assignments in adjacent cores, respectively. Since *Cores* 1 and 2 are non-adjacent,  $L_1$  and  $L_2$  can use overlapped spectra on them even though their trust-levels are different. Similarly, the Aa-RSCA solution in Fig. 1(d) also follows the operation principle we discussed above. This time, the lightpath pairs either occupy non-adjacent cores or use non-overlapped spectra with a guard-band in between on a same core, for minimizing crosstalk.

#### IV. ILP FORMULATION FOR STATIC PLANNING

In static network planning, we know the lightpath requests a priori and accommodate all of them in the SDM-EON with an Aa-RSCA algorithm, i.e., the spectrum resources are sufficient such that no request blocking would happen. In this scenario, the operator needs to determine how many FS' should be allocated on each core of the MCFs to improve spectrum utilization and reduce inter-core crosstalk as well. In this section, we formulate an ILP model for the optimization and analyze the intractability of the problem.

##### A. ILP Formulation

###### Parameters:

- $o$ : an integer to represent the index of an FS.

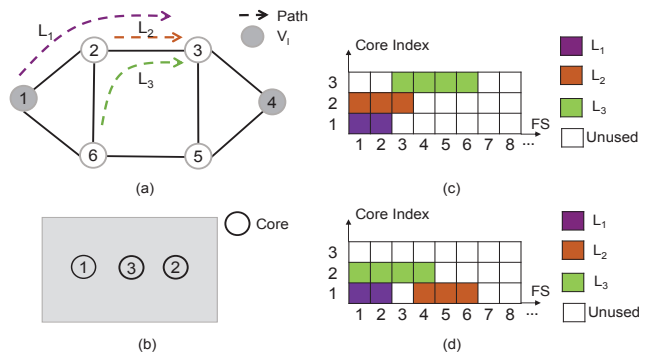


Fig. 1. Example on Aa-RSCA in an MCF-based SDM-EON, (a) network topology, (b) layout of a 3-core rectangular MCF, and (c) and (d) Aa-RSCA solutions on *Link* 2→3.

- $r_{i,j}$ : a boolean that equals 1 if  $L_i$  and  $L_j$  have different trust-levels, and 0 otherwise.
- $a^{u,v}$ : a boolean that equals 1 if cores  $u$  and  $v$  are adjacent, and 0 otherwise.
- $y_i^e$ : a boolean that equals 1 if the shortest routing path for  $L_i$  uses link  $e \in E$ , and 0 otherwise.
- $\eta_1, \eta_2$ : the weights that represent the importance of spectrum utilization and inter-core crosstalk, respectively.

###### Variables:

- $x_i^{u,e}$ : the boolean variable that equals 1 if  $L_i$  uses core  $u$  on link  $e$ , and 0 otherwise.
- $f_i, l_i$ : the integer variables that indicate the indices of the first/last FS' of the FS-block assigned to  $L_i$ , respectively.
- $st_{i,j}$ : the boolean variable that equals 1 if  $f_i < f_j$ , and 0 otherwise.
- $w_{i,o}, z_{i,o}$ : the boolean variables that equal 1 if  $o$  is no less than  $f_i$  or no more than  $l_i$ , and 0 otherwise, respectively.
- $p_{i,j}, q_{i,j}$ : the boolean variables that equal 1 if  $L_i$  and  $L_j$  use the same or neighboring core(s), and 0 otherwise, respectively.
- $b_{i,o}$ : the boolean variable that equals 1 if  $o$  is within the range of  $[f_i, l_i]$ , and 0 otherwise.
- $\varepsilon_o^{u,e}$ : the boolean variable that equals 1 if  $o$  is used on core  $u$  of link  $e$ , and 0 otherwise.
- $\rho_o^{u,v,e}$ : the boolean variable that equals 1 if  $o$  is used on cores  $u$  and  $v$  of link  $e$ , and 0 otherwise.
- $C$ : integer variable that indicates the total number of overlapped FS' on adjacent cores in the network, which can be used to quantify the total inter-core crosstalk.
- $F_m$ : the integer variable that indicates the maximum index of used FS' on all the cores in the network.

###### Objective:

Before formulating the objective, we provide two definitions related to spectrum utilization and inter-core crosstalk.

**Definition** The spectrum utilization can be represented with  $\overline{F}_m$ , which is normalized from  $F_m$  as

$$\overline{F}_m = \frac{F_m}{\sum_i n_i}. \quad (1)$$

**Definition** The average inter-core crosstalk  $\overline{C}$  can be quanti-

fixed as follows [15]

$$\bar{C} = \frac{C}{\sum_i n_i \cdot |P_i|}, \quad (2)$$

where  $|P_i|$  denotes the hop-count of  $P_i$ .

Then, the optimization objective can be formulated as

$$\text{Minimize } T = \eta_1 \cdot \bar{F}_m + \eta_2 \cdot \bar{C}, \quad (3)$$

where we set  $\eta_1 = \eta_2$  to make the two terms equally important in the joint optimization.

**Constraints:**

1) *Core Selection:*

$$\sum_{u=1}^N x_i^{u,e} = y_i^e, \quad \forall i, e. \quad (4)$$

Eq. (4) ensures that there is one and only one core selected on each link along the routing path for each lightpath.

2) *Spectrum Assignment:*

$$l_i - f_i + 1 = n_i, \quad f_i, l_i \in (0, F], \quad \forall i. \quad (5)$$

Eq. (5) ensures that each lightpath is set up with enough FS'.

$$st_{i,j} + st_{j,i} \leq 1, \quad \{i, j : i \neq j\}, \quad (6)$$

$$p_{i,j} \geq x_i^{u,e} + x_j^{u,e} - 1, \quad \{i, j, u, e : i \neq j\}, \quad (7)$$

$$l_j - f_i < F \cdot (1 + st_{i,j} - p_{i,j}), \quad \{i, j : i \neq j\}, \quad (8)$$

$$l_i - f_j < F \cdot (2 - st_{i,j} - p_{i,j}), \quad \{i, j : i \neq j\}. \quad (9)$$

Eqs. (6)-(9) ensure that if two lightpaths share the same core on link(s), their spectrum assignments should not overlap with each other or exceed the core's capacity.

$$\sum_{v \neq u} a^{u,v} \cdot x_j^{v,e} \leq q_{i,j} - x_i^{u,e} + 1, \quad \{i, j, u, e : i \neq j\}, \quad (10)$$

$$l_j - f_i < F \cdot (2 + st_{i,j} - q_{i,j} - r_{i,j}), \quad \{i, j : i \neq j\}, \quad (11)$$

$$l_i - f_j < F \cdot (3 - st_{i,j} - q_{i,j} - r_{i,j}), \quad \{i, j : i \neq j\}. \quad (12)$$

Eqs. (10)-(12) ensure that if two lightpaths with different trust-levels use neighboring cores on same link(s), their spectrum assignments should not overlap with each other or exceed the cores' capacity.

3) *Objective related Constraints:*

$$F_m \geq l_i, \quad F_m \in (0, F], \quad \forall i. \quad (13)$$

Eq. (13) determines the maximum index of used FS'.

$$w_{i,o} > \frac{o - f_i + 1}{F}, \quad z_{i,o} > \frac{l_i - o + 1}{F}, \quad \forall i, o. \quad (14)$$

$$b_{i,o} = w_{i,o} + z_{i,o} - 1, \quad \forall i, o. \quad (15)$$

$$\varepsilon_o^{u,e} \geq x_i^{u,e} + b_{i,o} - 1, \quad \forall i, o, u, e. \quad (16)$$

$$\rho_o^{u,v,e} \geq \varepsilon_o^{u,e} + \varepsilon_o^{v,e} - 1, \quad \forall o, u, v, e. \quad (17)$$

$$C = \sum_e \sum_{u=1}^N \sum_{v \neq u} \sum_{o=1}^F a^{u,v} \cdot \rho_o^{u,v,e}. \quad (18)$$

Eqs. (14)-(18) obtain the total inter-core crosstalk.

*B. Hardness Analysis*

**Theorem 1.** *The optimization problem described by the ILP formulation is NP-hard.*

*Proof:* In order to prove the NP-hardness of the optimization problem, we restrict away certain aspects of it until a known NP-hard problem appears [36]. Firstly, we set  $\eta_2 = 0$  to concentrate the optimization on spectrum utilization. Then, we can treat the cores in each MCF as parallel and independent fiber links, and the original optimization in Eq. 3 gets reduced to the generic spectrum assignment problem, which has already been proven to be NP-hard in [7]. Therefore, since the restricted case of our optimization problem is NP-hard, we prove its NP-hardness. ■

## V. HEURISTIC ALGORITHM FOR STATIC PLANNING

Due to its NP-hardness, we do not try to find an exact polynomial-time algorithm to solve the optimization in Eq. 3, but restore to designing a time-efficient heuristic. We design the heuristic to include three steps: 1) determining the provisioning order of the lightpath requests, 2) preprocessing available spectra in the network for each lightpath, and 3) provisioning the lightpaths. The detailed procedure of the steps will be discussed in the following subsections.

### A. Determine Provisioning Order

*Algorithm 1* explains how to sort the lightpath requests before provisioning them. *Lines 1-2* are for the initialization. In *Line 3*, we classify the pending lightpaths according to their trust-levels and store the trusted and untrusted ones in  $\Lambda^h$  and  $\Lambda^l$ , respectively. The while-loop that covers *Lines 4-14* sorts the lightpaths. Here, *Lines 5-6* select the lightpath request  $L_i$  whose bandwidth demand is the largest, and move it from  $\Lambda$  and  $\Lambda^h$  or  $\Lambda^l$  to  $\Omega$ . Then, *Lines 7-11* try to find the lightpaths whose trust-levels and routing paths are different from and link-joint with those of  $L_i$ , respectively. Next, *Lines 12-13* sort the found lightpaths and update  $\Omega$ ,  $\Lambda$ ,  $\Lambda^h$  and  $\Lambda^l$  accordingly. Finally, the sorted lightpaths are stored in set  $\mathbf{L}$  and returned in *Lines 15-16*. The complexity of *Algorithm 1* is  $O(|\mathbf{L}|)$ .

### B. Preprocess Spectrum Resources

**Definition** We define  $F_{m_i}$  as the maximum index of used FS' along the routing path for  $L_i$ , i.e.,  $P_i$ .

Since the operation principle of Aa-RSCA requires to avoid assigning overlapped spectra in neighboring cores to lightpaths in different trust-levels, we apply *Algorithm 2* to exclude the FS' that are available but should not be assigned to a lightpath according to this principle. *Line 1* initializes  $F_{m_i}$ . The two for-loops that cover *Lines 2-15* deal with each core on each link on  $P_i$ . For a core  $u$  on link  $e$ , *Lines 4-7* record the maximum index of used FS' on it and update  $F_{m_i}$  accordingly if necessary. After obtaining the neighboring cores of core  $u$  in *Line 8*, we use the inner for-loop covering *Lines 9-13* to check each neighboring core and mark the FS' that have been occupied by lightpaths whose trust-levels are different from that of  $L_i$  as unavailable. Finally, *Line 16* returns the output.

**Algorithm 1:** Determine Provisioning Order

---

**input** : Lightpath request set  $\mathbf{L}$ , routing path set  $\mathbf{P}$ .  
**output**: Set  $\mathbf{L}$  of lightpath requests in sorted order.

- 1  $\Lambda = \mathbf{L}$ ;
- 2  $\Omega = \emptyset$ ;
- 3 classify lightpaths in  $\Lambda$  into sets  $\Lambda^h$  and  $\Lambda^l$ ;
- 4 **while**  $|\Lambda| > 0$  **do**
- 5     select lightpath  $L_i$  with the largest bandwidth demand in  $\Lambda$ ;
- 6     insert  $L_i$  into  $\Omega$  and update  $\Lambda$ ,  $\Lambda^h$  and  $\Lambda^l$  to remove it;
- 7     **if**  $L_i \in \Lambda^h$  **then**
- 8         find the lightpaths in  $\Lambda^l$  whose routing paths are link-joint with that of  $L_i$ ;
- 9     **else**
- 10        find the lightpaths in  $\Lambda^h$  whose routing paths are link-joint with that of  $L_i$ ;
- 11     **end**
- 12     sort the found lightpaths in descending order of their bandwidth demands;
- 13     insert the sorted lightpaths into  $\Omega$  and update  $\Lambda$ ,  $\Lambda^h$  and  $\Lambda^l$  to remove them;
- 14 **end**
- 15  $\mathbf{L} = \Omega$ ;
- 16 **return**  $\mathbf{L}$ .

---

The complexity of *Lines* 4-8 is  $O(F + N)$ , where  $N$  is the number of cores on each MCF, and the for-loop covering *Lines* 9-13 has the complexity of  $O(N \cdot F)$  in the worst case. Hence, the complexity of *Algorithm 2* is  $O(|P_i| \cdot N^2 \cdot F)$ .

### C. Provision Lightpaths with Aa-RSCA

*Algorithm 3* shows the overall procedure of provisioning lightpath requests in static network planning. *Line* 1 is for the initialization. After determining the provisioning order in *Line* 2, we use the for-loop that covers *Lines* 3-29 to handle all the lightpath requests sequentially. For each lightpath request  $L_i$ , we first apply *Algorithm 2* to obtain  $F_{m_i}$  and the updated spectrum usage. Then, *Line* 5 initializes  $\Phi$ , which is used to store the feasible Aa-RSCA solutions for  $L_i$ . The for-loop covering *Lines* 6-26 prepares  $|F_{m_i} + 1|$  FS-block candidates, i.e.,  $\{[1, n_i], [2, n_i + 1], \dots, [F_{m_i} + 1, F_{m_i} + n_i]\}$ . Specifically, for each candidate  $[o, o + n_i - 1]$ ,  $o \in [1, F_{m_i} + 1]$ , the for-loop that covers *Lines* 9-20 checks whether its is available on each link along  $P_i$ . If yes, we select the first core on which the FS-block is available and store it in  $\Phi_o$ . In *Lines* 21-25, if a core is selected on each link along  $P_i$  (i.e.,  $|\Phi_o| = |P_i|$ ), we combine  $\Phi_o$  and FS-block  $[o, o + n_i - 1]$  as a feasible Aa-RSCA solution, and store it in  $\Phi$  with a weight  $\omega_o$ , which is defined as

$$\omega_o = \alpha \cdot \delta + \beta \cdot \sum_{\Phi_o} C_o^{u,e}, \quad (19)$$

where the value of  $\delta$  is obtained by a piecewise function

$$\delta = \begin{cases} 0, & o + n_i - 1 \leq F_{m_i}, \\ (o + n_i - 1) - F_{m_i}, & \text{otherwise,} \end{cases} \quad (20)$$

**Algorithm 2:** Preprocess Spectrum Resources

---

**input** : Lightpath request  $L_i$ , routing path  $P_i$  for  $L_i$ , spectrum usage along  $P_i$ .  
**output**:  $F_{m_i}$ , updated spectrum usage along  $P_i$ .

- 1  $F_{m_i} = 0$ ;
- 2 **for each link**  $e \in P_i$  **do**
- 3     **for each core**  $u$  **on**  $e$  **do**
- 4         record the maximum index of used FS' on core  $u$  as  $\varphi$ ;
- 5         **if**  $\varphi > F_{m_i}$  **then**
- 6              $F_{m_i} = \varphi$ ;
- 7         **end**
- 8         get the neighboring cores of core  $u$ ;
- 9         **for each neighboring core**  $v$  **do**
- 10             get the spectrum usage on core  $v$ ;
- 11             find FS' occupied by lightpaths whose trust-levels are different from that of  $L_i$ ;
- 12             mark the corresponding FS' as unavailable on core  $u$ ;
- 13         **end**
- 14     **end**
- 15 **end**
- 16 **return**  $F_{m_i}$  and updated spectrum usage along  $P_i$ .

---

$\sum_{\Phi_o} C_o^{u,e}$  is the total crosstalk caused by the Aa-RSCA solution, and  $\alpha$  and  $\beta$  are the weighting coefficients for the two terms. With the assistance of  $\omega_o$ , we select the Aa-RSCA solution whose weight is the smallest to provision  $L_i$  and update the network status in *Lines* 27-28. The complexity of *Algorithm 3* can be analyzed as follows. *Lines* 9-20 will run at most  $N \cdot |P_i|$  times. The complexity of the for-loop that covers *Lines* 6-26 is  $O(F_{m_i} \cdot N \cdot |P_i|)$ . Then, by considering the complexities of *Algorithms* 1 and 2, we can obtain the complexity of *Algorithm 3* as  $O(|L| \cdot |P_i| \cdot N^2 \cdot F)$ .

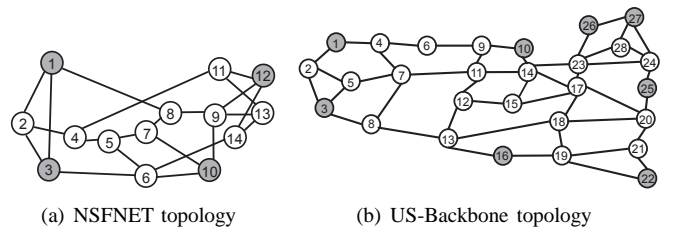


Fig. 2. Network topologies with untrusted nodes (i.e.,  $V_i$ ) marked in grey.

## VI. PERFORMANCE EVALUATION FOR STATIC PLANNING

### A. Simulation Setup

We evaluate the proposed algorithms for static network planning in three topologies, i.e., the six-node topology in Fig. 1(a) and the NSF and US-Backbone topologies in Fig. 2, and consider three types of MCFs, i.e., the 3-core MCF in Fig. 1(b) and the 7-core and 12-core MCFs in Fig. 3. More specifically, we assume that the six-node topology uses the 3-core and 7-core MCFs, while the other two topologies are deployed with

**Algorithm 3: Aa-RSCA for Static Network Planning**


---

```

input : Network topology  $G(V, E)$ , lightpath request
         set  $\mathbf{L}$ , routing path set  $\mathbf{P}$ .

1 initialize spectrum usage in  $G(V, E)$ ;
2 sort lightpath requests with Algorithm 1;
3 for  $i = 1$  to  $|\mathbf{L}|$  do
4   apply Algorithm 2 to obtain  $F_{m_i}$  and the updated
   spectrum usage for  $L_i$ ;
5    $\Phi = \{\Phi_o\}$ ;
6   for  $o = 1$  to  $F_{m_i} + 1$  do
7      $\Phi_o = \emptyset$ ;
8     get FS-block  $[o, o + n_i - 1]$ ;
9     for each link  $e \in P_i$  do
10      for each core  $u$  on  $e$  do
11        if FS-block  $[o, o + n_i - 1]$  is available
12         on core  $u$  then
13           calculate total crosstalk as  $C_o^{u,e}$ ;
14           store core  $u$  in  $\Phi_o$ ;
15           break;
16        end
17      if no feasible core is found then
18        break;
19      end
20    end
21    if  $|\Phi_o| = |P_i|$  then
22      combine  $\Phi_o$  and FS-block  $[o, o + n_i - 1]$ 
23      as a feasible Aa-RSCA solution;
24      assign weight  $\omega_o$  to the solution;
25      store the solution and its weight in  $\Phi$ ;
26    end
27  provision  $L_i$  using the solution with the smallest
  weight in  $\Phi$ ;
28  update network status;
29 end

```

---

the 7-core and 12-core MCFs. For each lightpath request, the source and destination are randomly selected from  $V$ , and its bandwidth demand is uniformly distributed within  $[1, 16]$  FS'. We denote our proposed heuristic as Aa-RSCA and adopt the first-fit and first-core based scheme (FF-FC) as the benchmark. The ILP model is solved by LINGO 11, while the heuristic is simulated with MATLAB R2011b. In the simulations, we get each data point by averaging the results from 50 independent simulations, which leads to an expected confidence level of 96% [37]. All the simulations run on a server with 2.20 GHz Intel Xeon E5-2420 CPU and 32 GB RAM.

### B. Simulation Results in Six-node Topology

Table I shows the results of the three algorithms. Here,  $T$  is the value of the optimization objective in Eq. (3), and  $F_m$  is the maximum index of used FS'. When 3-core MCFs are used in the SDM-EON, the ILP provides the smallest  $T$  when there are 5 and 10 pending lightpaths to be provisioned, as expected.

However, due to the high complexity, the ILP cannot obtain the optimal solution when there are 15 lightpath requests within a reasonable long time period (*i.e.*, five hours in this case). On the contrary, the running time of the two heuristics is much shorter and thus they are much more time-efficient. We also notice that our proposed Aa-RSCA achieves similar performance on  $T$  when being compared to the ILP, and outperforms FF-FC in terms of  $T$ . Regarding  $F_m$ , we observe that Aa-RSCA performs similarly as FF-FC and better than the ILP. Hence, the results verify that Aa-RSCA can balance spectrum utilization and inter-core crosstalk-level well. As for the SDM-EON based on 7-core MCFs, it can be seen that the simulation results follow the similar trends. In general, the results on  $T$  and  $F_m$  can be smaller than their counterparts in the SDM-EON based on 3-core MCFs, which is because each 7-core MCF includes more non-adjacent core pairs.

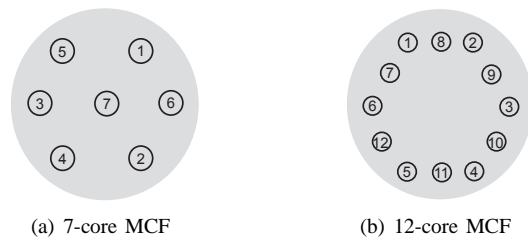


Fig. 3. Layouts of MCFs.

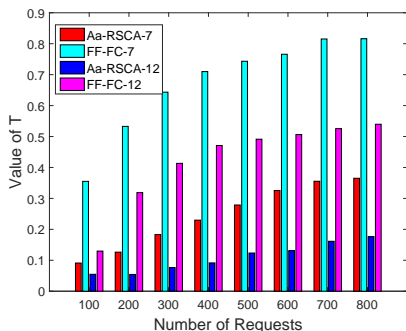
### C. Simulation Results in Large-scale Topologies

The simulation results obtained with the NSFNET topology are shown in Fig. 4. Here, we include the number of MCF cores in each algorithm's name, and for instance, "Aa-RSCA-7" means that the results are obtained by simulating Aa-RSCA in an SDM-EON based on 7-core MCFs. In Fig. 4(a), we can clearly see that compared with FF-FC, our proposed Aa-RSCA always achieves smaller  $T$ , no matter what type of MCFs are used. Then, Figs. 4(b) and 4(c) compare the algorithms in terms of the two metrics that contribute to  $T$ , *i.e.*, the average crosstalk  $\bar{C}$  and the maximum index of used FS'  $F_m$ . The results in Fig. 4(b) indicate that Aa-RSCA achieves much lower average crosstalk than FF-FC, while Fig. 4(c) verifies that Aa-RSCA's performance on  $F_m$  is comparable to that of FF-FC. For example, in the worst case, Aa-RSCA-12 increases  $F_m$  by 21.5% when there are 400 pending lightpaths, but it reduces  $\bar{C}$  by 83.0% at the same time. Hence, the results confirm that Aa-RSCA can balance the tradeoff between spectrum utilization and inter-core crosstalk better than the benchmark. Meanwhile, by comparing the results for SDM-EONs based on different MCFs, we can see that both algorithms perform better in the SDM-EON based on 12-core MCFs. This is because compared with a 7-core MCF, a 12-core one provides more spatial channels and its structure ensures that more non-adjacent core pairs can be found. Fig. 5 illustrates the results in the US-Backbone topology, which exhibit the similar trends as those in the NSFNET topology.

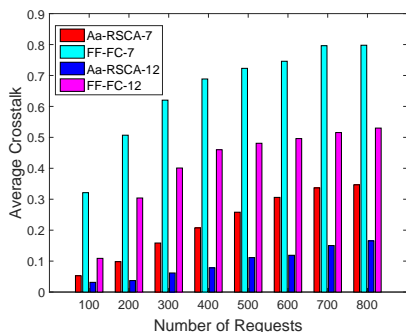
To further evaluate the algorithms, we also consider the scenarios in which none or 50% of the nodes in an SDM-EON are untrusted. The simulations are performed with the

TABLE I  
SIMULATION RESULTS IN SIX-NODE TOPOLOGY.

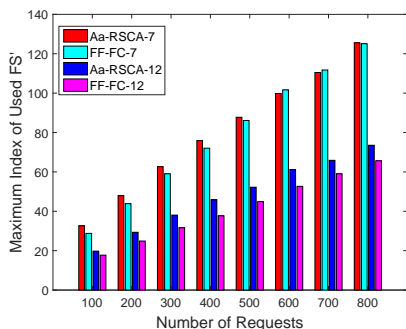
# of Lightpath Requests		5			10			15		
Algorithms		ILP	Aa-RSCA	FF-FC	ILP	Aa-RSCA	FF-FC	ILP	Aa-RSCA	FF-FC
3-core MCF	$T$	0.331	0.331	0.331	0.202	0.206	0.228	-	0.184	0.242
	$F_m$	13.8	13.8	13.8	17.0	16.8	16.7	-	18.6	18.4
	Running Time (s)	3.729	0.009	0.007	722.578	0.014	0.010	-	0.024	0.016
7-core MCF	$T$	0.331	0.331	0.331	0.187	0.189	0.197	-	0.139	0.165
	$F_m$	13.8	13.8	13.8	15.6	15.3	15.2	-	15.4	15.4
	Running Time (s)	11.082	0.010	0.007	343.187	0.019	0.010	-	0.031	0.014



(a) Value of  $T$ .

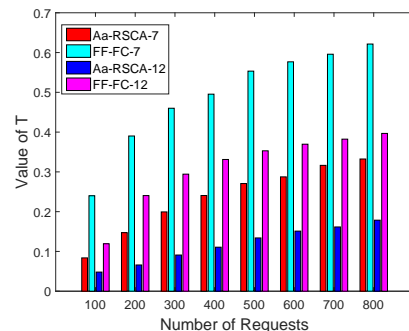


(b) Average crosstalk  $\bar{C}$ .

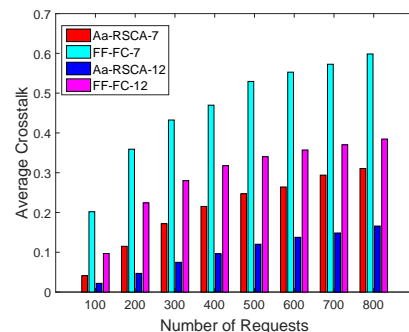


(c) Maximum index of used FS'  $F_m$ .

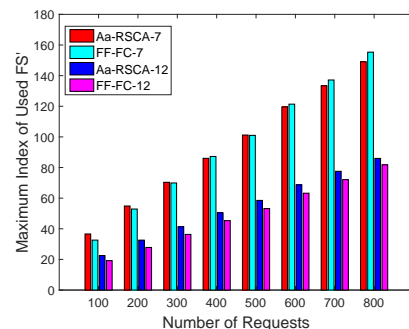
Fig. 4. Results of static planning in NSFNET topology.



(a) Value of  $T$ .



(b) Average crosstalk  $\bar{C}$ .



(c) Maximum index of used FS'  $F_m$ .

Fig. 5. Results of static planning in US-Backbone topology.

US-Backbone topologies in Fig. 6. The results are shown in Fig. 7 and Fig. 8, from which we can see that Aa-RSCA's effectiveness on balancing the tradeoff between spectrum utilization and inter-core crosstalk would not be affected by the percentage of untrusted nodes in the SDM-EON.

The advantage of Aa-RSCA over FF-FC can be understood as follows. For each lightpath request, Aa-RSCA finds several

feasible provisioning solutions and then selects the one that can balance the tradeoff between spectrum utilization and inter-core crosstalk in the best manner. Moreover, by sorting the lightpath requests beforehand intelligently, Aa-RSCA gives a higher priority to the lightpaths whose routing paths and trust-levels are link-joint with and different from those of the last provisioned one, respectively, to reduce  $F_m$ . On the other

hand, FF-FC always uses the first-fit scheme to select the FS-blocks and cores for lightpaths, which means that it concentrates too much on spectrum utilization. Therefore, although FF-FC can achieve a slightly lower  $F_m$  than Aa-RSCA, it performs much worse in terms of inter-core crosstalk.

## VII. DYNAMIC PROVISIONING

In this section, we consider the scenario of dynamic network provisioning, where the spectrum resources are limited and the lightpath requests can arrive and leave on-the-fly.

### A. Heuristic Algorithm

For dynamic network provisioning, our objective is changed to balance the tradeoff between blocking probability and inter-core crosstalk. It is known that in EONs, dynamic provisioning could generate spectrum fragmentation, which would result in high blocking probability [38]. Moreover, since the principle of Aa-RSCA might prevent us from using certain FS' even if they are unoccupied and available, the spectrum fragmentation could be further exacerbated. Therefore, we have to consider this issue when designing the Aa-RSCA algorithm for dynamic provisioning. In the following, we will incorporate the awareness of spectrum fragmentation in Aa-RSCA and come up with a heuristic for dynamic provisioning, namely, Aa-RSCA-D.

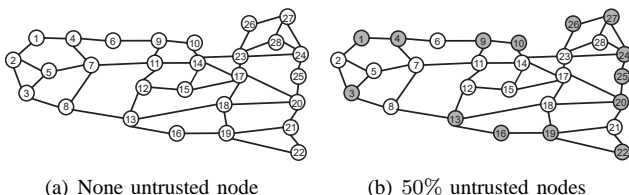
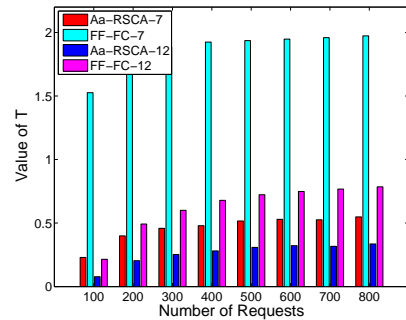


Fig. 6. US-Backbone with untrusted nodes (*i.e.*,  $V_i$ ) marked in grey.

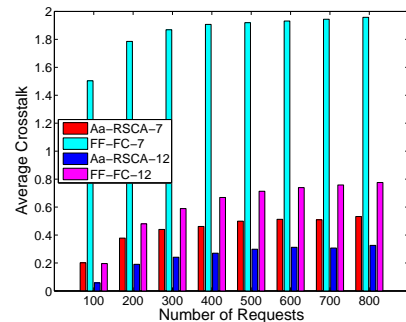
In each provision period, Aa-RSCA-D tries to serve all the pending lightpath requests. In general, the procedure of Aa-RSCA-D is similar as that of Aa-RSCA described in Section V. Specifically, we first determine the provisioning order for the pending requests. Here, Aa-RSCA-D tries to serve the requests in descending order of their bandwidth demands, since the lightpaths with larger bandwidth demands are more likely to be blocked when the network gets congested. Then, Aa-RSCA-D reuses most of the procedure in *Lines* 3-29 of *Algorithm* 3, with the exception that the weight  $\omega_o$  of each feasible solution is redefined as

$$\omega_o = \alpha \cdot \delta + \beta \cdot \rho + \gamma \cdot \sum_{\Phi_o} C_o^{u,e}, \quad (21)$$

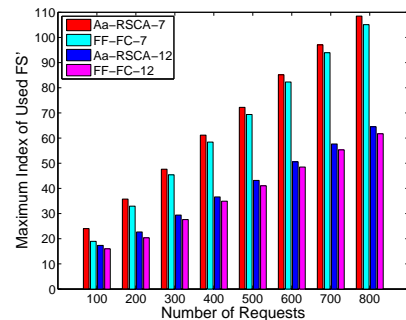
where  $\delta$  denotes the number of fragments that the solution will generate along the routing path, and  $\rho$  is to count how many in-service lightpaths whose trust-levels are different from the one to be provisioned use the FS-blocks that are spectrally-adjacent with the spectrum assignment of the solution on the same core of the same link. We introduce  $\rho$  because it would help to avoid the situation in which two or more lightpaths in different trust-levels adjoin making the overlapped spectra on neighboring cores unavailable for lightpaths whose trust-levels are different from theirs.  $\sum_{\Phi_o} C_o^{u,e}$  is the total crosstalk



(a) Value of  $T$ .



(b) Average crosstalk  $\bar{C}$ .



(c) Maximum index of used FS'  $F_m$ .

Fig. 7. Static planning in US-Backbone topology without untrusted nodes.

produced by the solution, while  $\alpha$ ,  $\beta$  and  $\gamma$  are the weighting coefficients to represent the importance of the terms.

### B. Performance Evaluation

The simulations are performed using the NSFNET and US-Backbone topologies equipped with the 7-core and 12-core MCFs in Fig. 3. For the topologies that are equipped with 7-core MCFs, we set the link capacity of each core as  $F = 358$  FS' (*i.e.*, corresponding to 4.475 THz optical spectra in the C-band if we assume that the bandwidth of each FS is 12.5 GHz), while for those using 12-core MCFs, we have  $F = 275$  FS'<sup>2</sup>. The lightpath requests arrive and leave dynamically following the Poisson traffic model that has an average arrival rate of  $\lambda$  per provision period, and their holding time follows

<sup>2</sup>Note that, for the topologies with 12-core MCFs, the blocking probability would be much lower under the same traffic load if we still set  $F = 358$  FS', since the actual spectrum resources in the networks become more. Hence, we reduce  $F$  to 275 in the topologies with 12-core MCFs, just for making it easier to organize the blocking probability results for the topologies with 7-core and 12-core MCFs in a same figure.



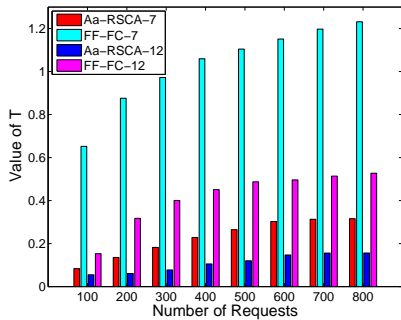
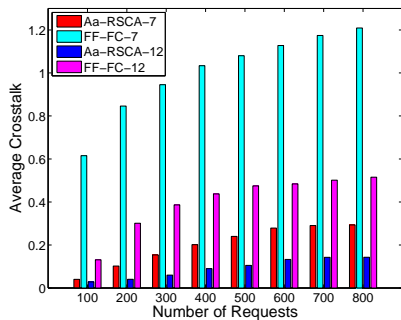
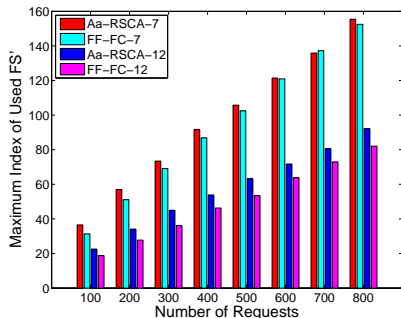
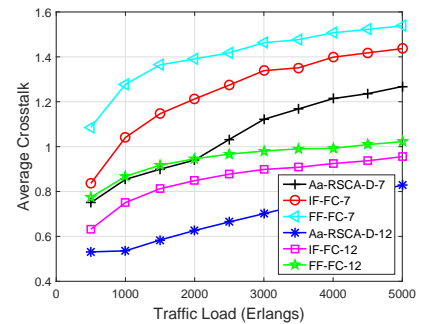
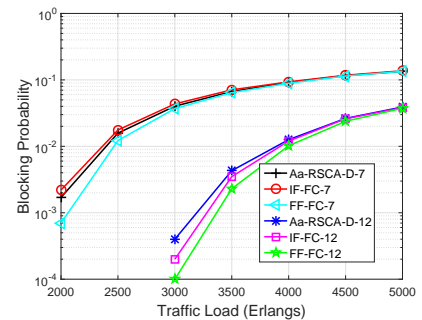
(a) Value of  $T$ .(b) Average crosstalk  $\bar{C}$ .(c) Maximum index of used FS'  $F_m$ .

Fig. 8. Static planning in US-Backbone topology with 50% untrusted nodes.

the negative exponential distribution with an average of  $\frac{1}{\mu}$  provision periods. Hence, the traffic load can be quantified as  $\frac{\lambda}{\mu}$  in Erlangs. The other simulation parameters are the same as those in the static planning. Besides FF-FC, we also adopt the algorithm developed in [14] as a benchmark and denote it as IF-FC, which realizes spectrum assignment based on prioritized areas. Similar as those in the static planning, we include the number of MCF cores in the name of each simulated algorithm, e.g., ‘‘Aa-RSCA-D-7’’ means that the results are obtained by simulating Aa-RSCA-D in an SDM-EON equipped with 7-core MCFs.

Fig. 9 shows the results in the NSFNET topology. In Fig. 9(a), it can be seen clearly that our proposed Aa-RSCA-D always provides the lowest average crosstalk  $\bar{C}$  regardless of the MCFs’ types. This attributes to the fact that for each lightpath request, Aa-RSCA-D prepares several feasible provisioning schemes and evaluates each of them with consideration of the crosstalk before selecting one. As for FF-FC, its average crosstalk is the highest because it always uses the first-fit

(a) Average crosstalk  $\bar{C}$ .

(b) Blocking probability.

Fig. 9. Results of dynamic provisioning in NSFNET topology.

TABLE II  
RUNNING TIME PER REQUEST IN NSFNET TOPOLOGY.

Traffic (Erlangs)	Running Time (s)		
	Aa-RSCA-D-7 / -12	IF-FC-7 / -12	FF-FC-7 / -12
500	0.009 / 0.009	0.003 / 0.003	0.005 / 0.005
1500	0.019 / 0.017	0.005 / 0.005	0.009 / 0.008
2500	0.020 / 0.021	0.007 / 0.007	0.012 / 0.011
3500	0.021 / 0.023	0.008 / 0.008	0.014 / 0.014
4500	0.021 / 0.024	0.009 / 0.009	0.015 / 0.016

scheme in the core and spectrum assignments, which would lead to grouping lightpaths in adjacent cores with the highest probability. IF-FC performs better than FF-FC but worse than Aa-RSCA-D in terms of the average crosstalk. This can be explained as follows. IF-FC first prioritizes the spectra into specific areas according to the bandwidth demands, which would help to separate the lightpaths to some extent. However, within each spectrum area, it still uses the first-fit scheme for spectrum assignment as FF-FC does. Meanwhile, all the three algorithms achieve lower average crosstalk in the topology equipped with 12-core MCFs.

Fig. 9(b) shows the results on blocking probability. We observe that no matter which the type of MCFs’ is used in the SDM-EON, Aa-RSCA-D achieves comparable blocking probability to that from IF-FC but performs slightly worse than FF-FC. This is reasonable because Aa-RSCA-D tries to balance the tradeoff between the blocking probability and inter-core crosstalk, while the two benchmarks concentrate more on the former. Note that, when comparing the two benchmarks, we notice that FF-FC outperforms IF-FC in terms of the blocking probability. This is because in our problem,

the operator has to strictly avoid the spectrum overlapping between lightpaths in different trust-levels. This would disturb the spectrum alignment in each area for specified bandwidth demands, *i.e.*, resulting in unwanted spectrum fragmentation, and thus make IF-FC inefficient. The running time of the algorithms are listed in Table II, which suggests that Aa-RSCA-D takes slightly longer time to provision a lightpath than the benchmarks, since its procedure is more sophisticated. Fig. 10 and Table III illustrate the results in the US-Backbone topology, which exhibit the similar trends as those in the NSFNET topology. Meanwhile, Fig. 11 and Fig. 12 plot the results of dynamic provisioning in US-Backbone topologies in which none and 50% of the nodes are untrusted, respectively. In all, the simulation results verify that compared with the existing crosstalk-aware RSCA schemes, our proposed Aa-RSCA-D can balance the tradeoff between blocking probability and inter-core crosstalk better in all the simulation scenarios.

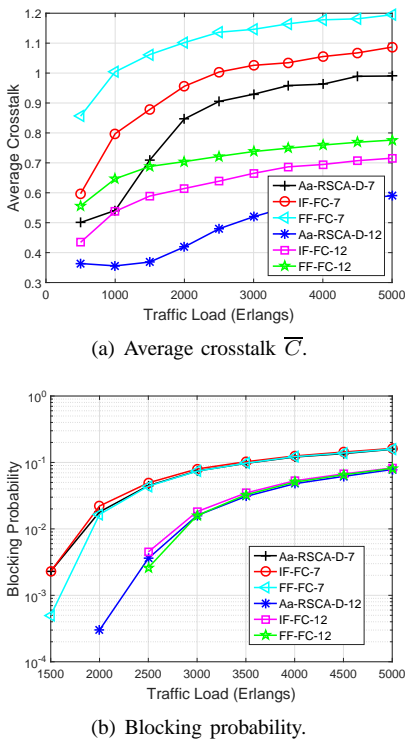


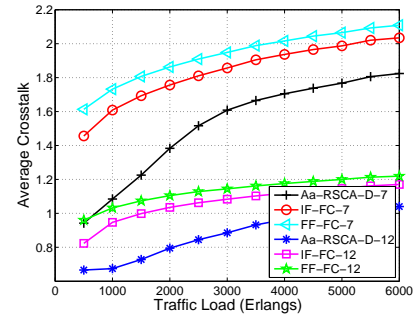
Fig. 10. Results of dynamic provisioning in US-Backbone topology.

TABLE III  
RUNNING TIME PER REQUEST IN US-BACKBONE TOPOLOGY.

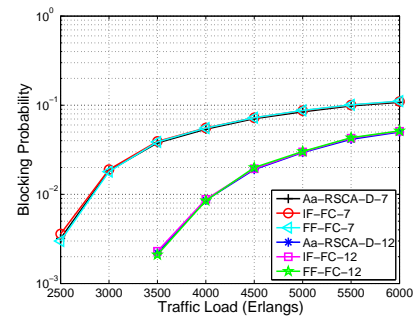
Traffic (Erlangs)	Running Time (s)		
	Aa-RSCA-D-7 / -12	IF-FC-7 / -12	FF-FC-7 / -12
500	0.021 / 0.017	0.005 / 0.005	0.007 / 0.007
1500	0.027 / 0.028	0.007 / 0.007	0.012 / 0.012
2500	0.028 / 0.031	0.010 / 0.009	0.016 / 0.016
3500	0.028 / 0.033	0.012 / 0.011	0.018 / 0.018
4500	0.031 / 0.036	0.013 / 0.013	0.020 / 0.020

## VIII. CONCLUSION

In this paper, we considered an MCF-based SDM-EON in which certain nodes have a lower trust-level than others, and

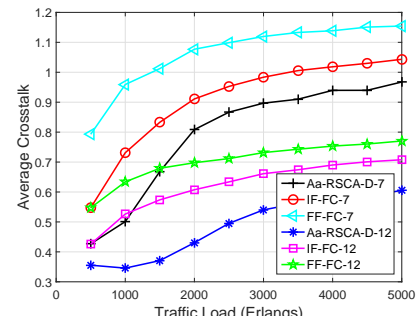


(a) Average crosstalk  $\bar{C}$ .

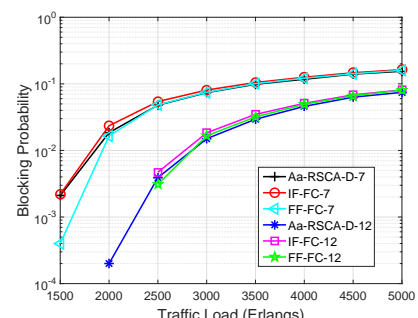


(b) Blocking probability.

Fig. 11. Dynamic provisioning in US-Backbone without untrusted nodes.



(a) Average crosstalk  $\bar{C}$ .



(b) Blocking probability.

Fig. 12. Dynamic provisioning in US-Backbone with 50% untrusted nodes.

studied how to provision lightpaths in such a network with consideration of the inter-core crosstalk related impairments and security issues. Both static network planning and dynamic network provisioning scenarios were investigated. For static planning, we first formulated an ILP model to optimize the spectrum utilization and inter-core crosstalk level jointly, and then proposed a time-efficient heuristic, namely, Aa-RSCA.

Simulation results confirmed that in a small-scale network, Aa-RSCA could approximate the ILP's performance with much higher time-efficiency. Meanwhile, compared with an existing benchmark, it could balance the tradeoff between spectrum utilization and inter-core crosstalk better. For dynamic provisioning, we tried to balance the tradeoff between blocking probability and inter-core crosstalk, and modified Aa-RSCA as Aa-RSCA-D. Simulation results verified that Aa-RSCA-D can balance the tradeoff better than two existing benchmark algorithms, *i.e.*, it achieved much lower average inter-core crosstalk while providing comparable blocking probability.

#### ACKNOWLEDGMENTS

This work was supported in part by the NSFC Project 61371117, the Key Project of the CAS (QYZDY-SSW-JSC003), and the NGBWMCN Key Project under Grant No. 2017ZX03001019-004.

#### REFERENCES

- [1] P. Lu *et al.*, "Highly-efficient data migration and backup for big data applications in elastic optical inter-datacenter networks," *IEEE Netw.*, vol. 29, pp. 36–42, Sept./Oct. 2015.
- [2] Z. Zhu, W. Lu, L. Zhang, and N. Ansari, "Dynamic service provisioning in elastic optical networks with hybrid single-/multi-path routing," *J. Lightw. Technol.*, vol. 31, pp. 15–22, Jan. 2013.
- [3] W. Shi, Z. Zhu, M. Zhang, and N. Ansari, "On the effect of bandwidth fragmentation on blocking probability in elastic optical networks," *IEEE Trans. Commun.*, vol. 61, pp. 2970–2978, Jul. 2013.
- [4] L. Gong and Z. Zhu, "Virtual optical network embedding (VONE) over elastic optical networks," *J. Lightw. Technol.*, vol. 32, pp. 450–460, Feb. 2014.
- [5] G. Saridis, D. Alexandropoulos, G. Zervas, and D. Simeonidou, "Survey and evaluation of space division multiplexing: From technologies to optical networks," *IEEE Commun. Surveys Tuts.*, vol. 17, pp. 2136–2156, Fourth Quarter 2015.
- [6] T. Kobayashi *et al.*, "1-Pb/s (32 SDM/46 WDM/768 Gb/s) C-band dense SDM transmission over 205.6-km of single-mode heterogeneous multi-core fiber using 96-Gbaud PDM-16QAM channels," in *Proc. of OFC 2017*, pp. 1–3, Mar. 2017.
- [7] Y. Wang, X. Cao, and Y. Pan, "A study of the routing and spectrum allocation in spectrum-sliced elastic optical path networks," in *Proc. of INFOCOM 2011*, pp. 1503–1511, Apr. 2011.
- [8] L. Gong, X. Zhou, W. Lu, and Z. Zhu, "A two-population based evolutionary approach for optimizing routing, modulation and spectrum assignments (RMSA) in O-OFDM networks," *IEEE Commun. Lett.*, vol. 16, pp. 1520–1523, Sept. 2012.
- [9] W. Lu and Z. Zhu, "Dynamic service provisioning of advance reservation requests in elastic optical networks," *J. Lightw. Technol.*, vol. 31, pp. 1621–1627, May 2013.
- [10] L. Gong *et al.*, "Efficient resource allocation for all-optical multicasting over spectrum-sliced elastic optical networks," *J. Opt. Commun. Netw.*, vol. 5, pp. 836–847, Aug. 2013.
- [11] L. Zhang and Z. Zhu, "Spectrum-efficient anycast in elastic optical inter-datacenter networks," *Opt. Switch. Netw.*, vol. 14, pp. 250–259, Aug. 2014.
- [12] Z. Zhu *et al.*, "Impairment- and splitting-aware cloud-ready multicast provisioning in elastic optical networks," *IEEE/ACM Trans. Netw.*, vol. 25, pp. 1220–1234, Apr. 2017.
- [13] L. Zhang, N. Ansari, and A. Khreishah, "Anycast planning in space division multiplexing elastic optical networks with multi-core fibers," *IEEE Commun. Lett.*, vol. 20, pp. 1983–1986, Oct. 2016.
- [14] H. Tode and Y. Hirota, "Routing, spectrum, and core and/or mode assignment on space-division multiplexing optical networks," *J. Opt. Commun. Netw.*, vol. 9, pp. A99–A113, Jan. 2017.
- [15] S. Fujii, Y. Hirota, H. Tode, and K. Murakami, "On-demand spectrum and core allocation for reducing crosstalk in multicore fibers in elastic optical networks," *J. Opt. Commun. Netw.*, vol. 6, pp. 1059–1071, Dec. 2014.
- [16] N. Skorin-Kapov, M. Furdek, S. Zsigmond, and L. Wosinska, "Physical-layer security in evolving optical networks," *IEEE Commun. Mag.*, vol. 54, pp. 110–117, Aug. 2016.
- [17] N. Skorin-Kapov, J. Chen, and L. Wosinska, "A new approach to optical networks security: Attack-aware routing and wavelength assignment," *IEEE/ACM Trans. Netw.*, vol. 18, pp. 750–760, Jun. 2010.
- [18] J. Zhu, B. Zhao, W. Lu, and Z. Zhu, "Attack-aware service provisioning to enhance physical-layer security in multi-domain EONs," *J. Lightw. Technol.*, vol. 34, pp. 2645–2655, Jun. 2016.
- [19] Y. Yin *et al.*, "Spectral and spatial 2D fragmentation-aware routing and spectrum assignment algorithms in elastic optical networks," *J. Opt. Commun. Netw.*, vol. 5, pp. A100–A106, Oct. 2013.
- [20] M. Zhang, C. You, H. Jiang, and Z. Zhu, "Dynamic and adaptive bandwidth defragmentation in spectrum-sliced elastic optical networks with time-varying traffic," *J. Lightw. Technol.*, vol. 32, pp. 1014–1023, Mar. 2014.
- [21] W. Fang *et al.*, "Joint defragmentation of optical spectrum and IT resources in elastic optical datacenter interconnections," *J. Opt. Commun. Netw.*, vol. 7, pp. 314–324, Mar. 2015.
- [22] Y. Shen, K. Lu, and W. Gu, "Coherent and incoherent crosstalk in WDM optical networks," *J. Lightw. Technol.*, vol. 17, pp. 759–764, May 1999.
- [23] R. Rejeb, M. Leeson, and R. Green, "Fault and attack management in all-optical networks," *IEEE Commun. Mag.*, vol. 44, pp. 79–86, Nov. 2006.
- [24] Y. Du, F. Xue, and B. Yoo, "Security enhancement of SPECTS O-CDMA through concealment against upstream DPSK eavesdropping," *J. Lightw. Technol.*, vol. 25, pp. 2799–2806, Sept. 2007.
- [25] Z. Zhu *et al.*, "Jitter and amplitude noise accumulations in cascaded all-optical regenerators," *J. Lightw. Technol.*, vol. 26, pp. 1640–1652, Jun. 2008.
- [26] M. Fok, Z. Wang, Y. Deng, and P. Prucnal, "Optical layer security in fiber-optic networks," *IEEE Trans. Inf. Forensics Security*, vol. 6, pp. 725–736, Sept. 2011.
- [27] N. Skorin-Kapov and M. Furdek, "Limiting the propagation of intra-channel crosstalk attacks in optical networks through wavelength assignment," in *Prof. of OFC 2009*, pp. 1–3, Mar. 2009.
- [28] M. Furdek, N. Skorin-Kapov, and M. Grbac, "Attack-aware wavelength assignment for localization of in-band crosstalk attack propagation," *J. Opt. Commun. Netw.*, vol. 2, pp. 1000–1009, Nov. 2010.
- [29] K. Manousakis and G. Ellinas, "Attack-aware planning of transparent optical networks," *Opt. Switch. Netw.*, vol. 19, pp. 97–109, 2016.
- [30] J. Zhu, B. Zhao, and Z. Zhu, "Leveraging game theory to achieve efficient attack-aware service provisioning in EONs," *J. Lightw. Technol.*, vol. 35, pp. 1785–1796, May 2017.
- [31] M. Koshiha, K. Saitoh, K. Takenaga, and S. Matsuo, "Multi-core fiber design and analysis: coupled-mode theory and coupled-power theory," *Opt. Express*, vol. 19, pp. B102–B111, Dec. 2011.
- [32] A. Muhammad, G. Zervas, D. Simeonidou, and R. Forchheimer, "Routing, spectrum and core allocation in flexgrid SDM networks with multi-core fibers," in *Proc. of ONDM 2014*, pp. 192–197, May 2014.
- [33] W. Lu *et al.*, "Dynamic multi-path service provisioning under differential delay constraint in elastic optical networks," *IEEE Commun. Lett.*, vol. 17, pp. 158–161, Jan. 2013.
- [34] F. Ji *et al.*, "Dynamic p-cycle protection in spectrum-sliced elastic optical networks," *J. of Lightw. Technol.*, vol. 32, pp. 1190–1199, Mar. 2014.
- [35] W. Lu and Z. Zhu, "Malleable reservation based bulk-data transfer to recycle spectrum fragments in elastic optical networks," *J. Lightw. Technol.*, vol. 33, pp. 2078–2086, May 2015.
- [36] M. Garey and D. Johnson, *Computers and Intractability: a Guide to the Theory of NP-Completeness*. W. H. Freeman & Co. New York, 1979.
- [37] S. Buckland, "Monte carlo confidence intervals," *Biometrics*, vol. 40, pp. 811–817, Sept. 1984.
- [38] M. Zhang, C. You, and Z. Zhu, "On the parallelization of spectrum defragmentation reconfigurations in elastic optical networks," *IEEE/ACM Trans. Netw.*, vol. 24, pp. 2819–2833, Oct. 2016.